



Electrochemical, EPR and computational results on $[\text{Fe}_2\text{Cp}_2(\text{CO})_2]$ -based complexes with a bridging hydrocarbyl ligand

Adriano Boni^{a,b}, Tiziana Funaioli^a, Fabio Marchetti^{a,*}, Guido Pampaloni^a, Calogero Pinzino^c, Stefano Zacchini^d

^a University of Pisa, Dipartimento di Chimica e Chimica Industriale, Via Risorgimento 35, 56126 Pisa, Italy

^b Scuola Normale Superiore, Piazza dei Cavalieri, I-56126 Pisa, Italy

^c ICCOM-CNR UOS, Area della Ricerca, Via Moruzzi 1, 56124 Pisa (I), Italy

^d University of Bologna, Dipartimento di Chimica Fisica e Inorganica, Viale Risorgimento 4, 40136 Bologna, Italy

ARTICLE INFO

Article history:

Received 29 June 2011

Received in revised form

27 July 2011

Accepted 29 July 2011

Keywords:

Diiron complexes

Dimetallacyclopentenone complexes

Allenyl ligand

Vinyl ligand

Electrochemistry

DFT calculations

ABSTRACT

The dimetallacyclopentenone complexes $[\text{Fe}_2\text{Cp}_2(\text{CO})(\mu\text{-CO})\{\mu\text{-}\eta^1\text{:}\eta^3\text{-C}_\alpha\text{H}=\text{C}_\beta(\text{R})\text{C}(=\text{O})\}]$ ($\text{R} = \text{CH}_2\text{OH}$, **1a**; $\text{R} = \text{CMe}_2\text{OH}$, **1b**; $\text{R} = \text{Ph}$, **1c**) were prepared by photolytic reaction of $[\text{Fe}_2\text{Cp}_2(\text{CO})_4]$ with alkyne according to the literature procedure. The X-ray and the electrochemical characterization of **1c** are presented. The μ -allenyl compound $[\text{Fe}_2\text{Cp}_2(\text{CO})_2(\mu\text{-CO})\{\mu\text{-}\eta^1\text{:}\eta^2_{\alpha,\beta}\text{-C}_\alpha\text{H}=\text{C}_\beta=\text{CMe}_2\}][\text{BF}_4]$ (**2**)[BF_4], obtained by reaction of **1b** with HBF_4 , underwent monoelectron reduction to give a radical species which was detected by EPR at room temperature. The EPR signal has been assigned to $[\text{Fe}_2\text{Cp}_2(\text{CO})_2(\mu\text{-CO})\{\mu\text{-}\eta^1\text{:}\eta^2_{\alpha,\beta}\text{-C}_\alpha\text{H}=\text{C}_\beta=\text{CMe}_2\}]$, **2**[•]. The molecular structures of **2**⁺ and **2**[•] were optimized by DFT calculations. The unpaired electron in **2**[•] is localized mainly at the metal centers and, coherently, **2**[•] does not undergo carbon–carbon dimerization, by contrast with what previously observed for the μ -vinyl radical complex $[\text{Fe}_2\text{Cp}_2(\text{CO})_2(\mu\text{-CO})\{\mu\text{-}\eta^1\text{:}\eta^2\text{-CH}=\text{CH}(\text{Ph})\}]$ [•], **3**[•]. Electron spin density distributions similar to the one of **2**[•] were found for the μ -allenyl radical complexes $[\text{Fe}_2\text{Cp}_2(\text{CO})_2(\mu\text{-CO})\{\mu\text{-}\eta^1\text{:}\eta^2_{\alpha,\beta}\text{-C}_\alpha\text{H}=\text{C}_\beta=\text{C}(\text{R}^1)(\text{R}^2)\}]$ [•] ($\text{R}^1 = \text{R}^2 = \text{H}$, **4**[•]; $\text{R}^1 = \text{H}$, $\text{R}^2 = \text{Ph}$, **5**[•]; $\text{R}^1 = \text{R}^2 = \text{Ph}$, **6**[•]).

© 2011 Elsevier Ltd. All rights reserved.

1. Introduction

The reactivity of diiron complexes based on the $[\text{Fe}_2\text{Cp}_2(\text{-CO})(\mu\text{-CO})]$ core has been the object of intense investigation [1]. This metal frame may provide non conventional reactivity patterns to bridging hydrocarbyl ligands and offer the possibility of stabilizing coordination fashions, as consequence of the cooperativity effects of the two iron centers [2]. The long known reaction of $[\text{Fe}_2\text{Cp}_2(\text{CO})_4]$ with alkynes under UV irradiation results in removal of one carbonyl ligand and insertion of the alkyne into a Fe–CO bond [3]; this approach has allowed the synthesis of a variety of dimetallacyclopentenone compounds, including $[\text{Fe}_2\text{Cp}_2(\text{CO})(\mu\text{-CO})\{\mu\text{-}\eta^1\text{:}\eta^3\text{-C}_\alpha\text{H}=\text{C}_\beta(\text{R})\text{C}(=\text{O})\}]$ ($\text{R} = \text{CMe}_2\text{OH}$, **1b** [4]; $\text{R} = \text{Ph}$, **1c** [3]), see Scheme 1.

The chemistry of these derivatives is dominated by the $\text{C}_\beta\text{-CO}$ bond cleavage promoted by proton addition, which takes place selectively at different sites depending on the nature of R. In the case of **1b**, the protonation is addressed to the hydroxo group and leads to formation of the μ -allenyl species **2**[BF_4] via water removal [4,5],

see Scheme 1. Otherwise, in the case of **1c**, the proton attacks the C_β carbon yielding the μ -vinyl complex $[\text{Fe}_2\text{Cp}_2(\text{CO})_2(\mu\text{-CO})\{\mu\text{-}\eta^1\text{:}\eta^2\text{-C}_\alpha\text{H}=\text{C}_\beta\text{H}(\text{Ph})\}][\text{BF}_4]$ (**3**)[BF_4], Scheme 1 [6].

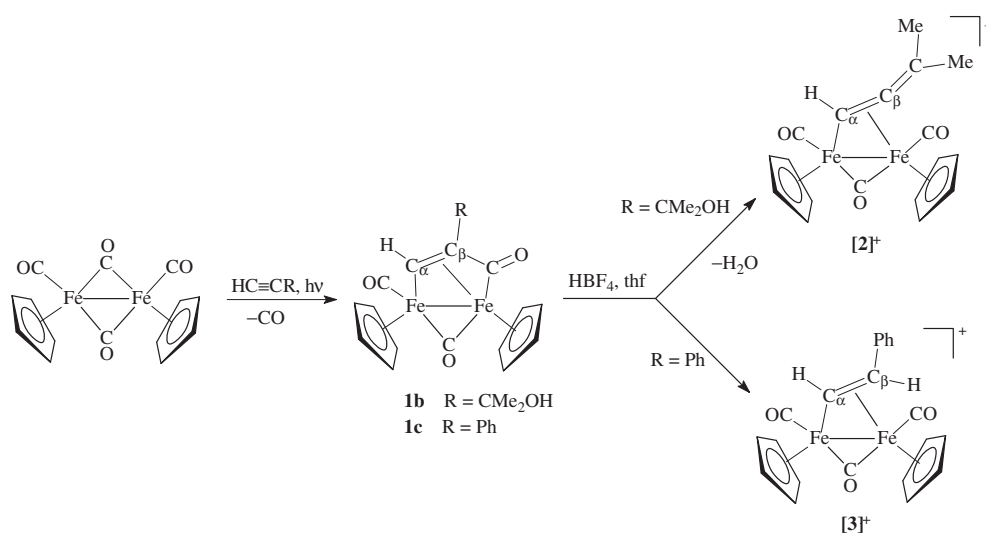
In a recent paper, we have outlined the unusual electrochemical behavior of **3**⁺, that undergoes reversible C–C dimerization upon monoelectron reduction [7]. We present herein some novel features regarding diiron complexes containing the $[\text{Fe}_2\text{Cp}_2(\text{CO})(\mu\text{-CO})]$ core: i) the preparation and the characterization of the unreported dimetallacyclopentenone compound $[\text{Fe}_2\text{Cp}_2(\text{CO})(\mu\text{-CO})\{\mu\text{-}\eta^1\text{:}\eta^3\text{-C}_\alpha\text{H}=\text{C}_\beta(\text{CH}_2\text{OH})\text{C}(=\text{O})\}]$ (**1a**); ii) the X-ray and the electrochemical characterization of the dimetallacyclopentenone $[\text{Fe}_2\text{Cp}_2(\text{CO})(\mu\text{-CO})\{\mu\text{-}\eta^1\text{:}\eta^3\text{-C}_\alpha\text{H}=\text{C}_\beta(\text{Ph})\text{C}(=\text{O})\}]$ (**1c**); iii) a detailed investigation on the electrochemistry of the μ -allenyl $[\text{Fe}_2\text{Cp}_2(\text{CO})_2(\mu\text{-CO})\{\mu\text{-}\eta^1\text{:}\eta^2_{\alpha,\beta}\text{-C}_\alpha\text{H}=\text{C}_\beta=\text{CMe}_2\}][\text{BF}_4]$ (**2**)[BF_4], including EPR and DFT analyses.

2. Results and discussion

The new compound $[\text{Fe}_2\text{Cp}_2(\text{CO})(\mu\text{-CO})\{\mu\text{-}\eta^1\text{:}\eta^3\text{-C}_\alpha\text{H}=\text{C}_\beta(\text{CH}_2\text{OH})\text{C}(=\text{O})\}]$ (**1a**) was prepared in moderate yield by photolytic reaction of $[\text{Fe}_2\text{Cp}_2(\text{CO})_4]$ with propargyl alcohol, according to the published procedure (Scheme 2) [3,4]. Compound **1a**, which

* Corresponding author.

E-mail address: fabmar@dcci.unipi.it (F. Marchetti).



Scheme 1.

adds to the family of analogous dimetallacyclopentenone complexes, has been characterized by IR and NMR spectroscopy, and elemental analysis. The IR spectrum (in the solid state) exhibits the absorptions due to terminal and bridging carbonyl ligands (1953 and 1787 cm^{-1} respectively), and one more absorption related to the acyl group (1744 cm^{-1}). Moreover a broad band at 3410 cm^{-1} accounts for the presence of the OH unit. The ^1H NMR spectrum (in CDCl_3) shows the resonance of the alkylidene proton at typical low field ($\delta = 12.16$ ppm). The signals in the ^{13}C NMR spectrum have been attributed as follows: δ 261.6 ($\text{CO}_{\text{bridging}}$), 235.2 (C=O), 210.3 ($\text{CO}_{\text{terminal}}$), 176.8 (C_α), 87.4, 85.8 (Cp), 77.2 (CH_2), 9.4 (C_β).

The reaction of **1a** with HBF_4 , performed under experimental conditions analogous to those employed for the protonation of **1b** (Scheme 1), failed to give cleanly the expected allenyl derivative $[\text{Fe}_2\text{Cp}_2(\text{CO})_2(\mu\text{-CO})\{\mu\text{-}\eta^1:\eta^2_{\alpha,\beta}\text{-C}_\alpha\text{H}=\text{C}_\beta=\text{CH}_2\}][\text{BF}_4]$, see Scheme 2 [8].

In view of our interest on the chemistry of the vinyl complex **[3]** $[\text{BF}_4]$ [7], we prepared the intermediate dimetallacyclopentenone $[\text{Fe}_2\text{Cp}_2(\text{CO})(\mu\text{-CO})\{\mu\text{-}\eta^1:\eta^3\text{-C}_\alpha\text{H}=\text{C}_\beta(\text{Ph})\text{C}(=\text{O})\}]$ (**1c**). In the course of the purification of this compound we collected some X-ray quality crystals, which were used for a X-ray diffraction analysis. The ORTEP molecular diagram of **1c** is shown in Fig. 1, whereas relevant bond lengths and angles are reported in Table 1.

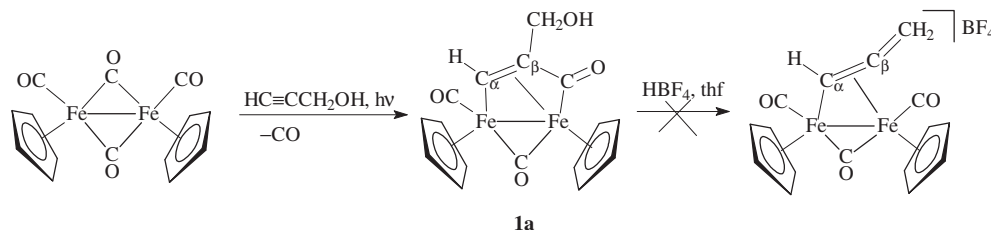
The molecular structure of **1c** closely resembles that previously reported for the analogous Ru-complex $[\text{Ru}_2\text{Cp}_2(\text{CO})(\mu\text{-CO})\{\mu\text{-}\eta^1:\eta^3\text{-C}_\alpha(\text{Ph})=\text{C}_\beta(\text{Ph})\text{C}(=\text{O})\}]$ **[3]**, so the former will be only briefly described here. Compound **1c** contains a bridging $\{\mu\text{-}\eta^1:\eta^3\text{-C}_\alpha\text{H}=\text{C}_\beta(\text{Ph})\text{C}(=\text{O})\}$ ligand coordinated to the *cis*- $\text{Fe}_2\text{Cp}_2(\text{CO})(\mu\text{-CO})$ core. The bonding of the bridging ligand can be formalized in terms of three resonance forms. The first form consists of a dimetallacyclopentenone ring $\text{Fe}(1)\text{-C}(13)\text{-C}(14)\text{-C}(15)\text{-Fe}(2)$, in which the

$\text{C}(13)\text{-C}(14)$ double bond is η^2 -bound to $\text{Fe}(2)$ (Scheme 3, form **I**). In the second form, $\text{C}(13)$ may be regarded as a μ -carbene with a ketenic substituent $[\text{C}(14)=\text{C}(15)=\text{O}(1)]$ which is η^2 -bonded to $\text{Fe}(2)$ through $\text{C}(14)\text{-C}(15)$ (Scheme 3, form **II**). A third description as an allylic ligand appears to have some validity (Scheme 3, form **III**), however the bonding parameters suggest that the actual situation may be represented almost exclusively by **I** and **II**, with prevalence of **I**. The $\text{C}(15)\text{-O}(1)$ interaction [1.210(10) Å] possesses an almost pure double bond character, whereas both $\text{C}(13)\text{-C}(14)$ [1.442(12) Å] and $\text{C}(14)\text{-C}(15)$ [1.463(12) Å] are in between a single and a double bond.

On account of the fact that scarce information is available in the literature regarding the electrochemical behavior of diiron complexes based on the $[\text{Fe}_2\text{Cp}_2(\text{CO})_2]$ core [9], we carried out electrochemical analysis on compound **1c** and on the allenyl complex **[2]** $[\text{BF}_4]$.

Compound **1c** undergoes two irreversible oxidation processes at +0.17 and +0.97 V (vs FeCp_2) and one reduction at -1.85 V, in $\text{CH}_2\text{Cl}_2/[\text{N}^i\text{Bu}_4][\text{PF}_6]$ solution. Analysis of the cyclic voltammograms, with scan rates varying between 0.02 and 1.00 V s^{-1} , have confirmed that the reduction is an electrochemically-reversible, diffusion-controlled process (the peak-to-peak separation, ΔE_p , approaches the theoretical value of 59 mV and the $(i_p)_{\text{red}}/v^{1/2}$ remains almost constant [10]), complicated by a subsequent fast chemical reaction ($i_{pc}/i_{pa} = 0.31$ at 1.0 V s^{-1}).

Fig. 2 shows the cyclic voltammetric profile exhibited by the allenyl complex **[2]** $[\text{BF}_4]$ in $\text{CH}_2\text{Cl}_2/[\text{N}^i\text{Bu}_4][\text{PF}_6]$ solution. Two irreversible oxidation (+1.11 and +1.48 V) and two consecutive reduction processes (-1.03 and -2.04 V) point out an electrochemical behavior similar to that of **[3]** $[\text{BF}_4]$ [7]. According to the cyclic voltammetric response of the reductions, with scan rates varying



Scheme 2.

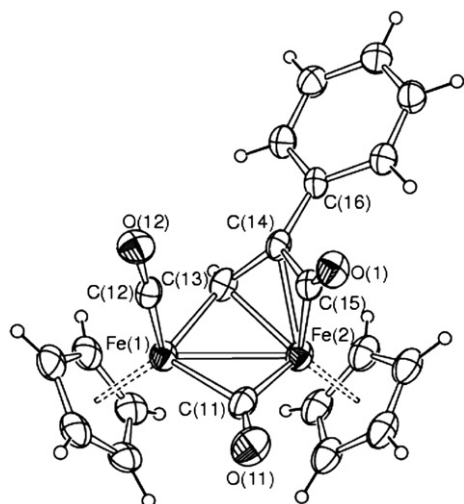


Fig. 1. Molecular structure of $[\text{Fe}_2\text{Cp}_2(\text{CO})(\mu\text{-CO})\{\mu\text{-}\eta^1:\eta^3\text{-C(H)=C(Ph)C(=O)}\}]$ (**1c**), with key atoms labeled. Thermal ellipsoids are at the 30% probability level. Only the main image of the disordered Cp bound to Fe(2) is drawn.

between 0.02 and 1.00 V s^{-1} , the first reduction is an electrochemically-reversible, diffusion-controlled process complicated by a subsequent chemical reaction ($i_{pc}/i_{pa} = 0.73$ at 0.10 V s^{-1}). This is testified by the appearance of oxidation processes in the back scan toward positive potentials, and by the deposition, after several cycles, of insoluble by-products onto the electrode surface.

The reduction process occurring at the more negative potential (−2.04 V) appears as a quasi-reversible one (Fig. 2).

The gas phase structure of the allenyl complex $[\mathbf{2}]^+$ and that of $[\mathbf{2}]^*$, which is the formal product of the mono-electron reduction of $[\mathbf{2}]^+$, were optimized by DFT calculations (the calculated structure of $[\mathbf{2}]^+$ is shown in Fig. 3).

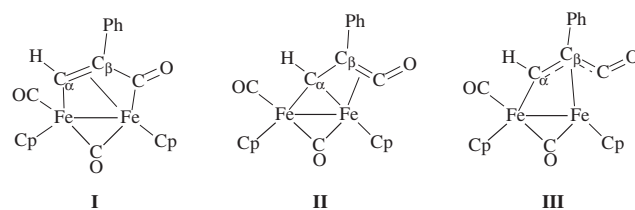
EPR experiment was carried out at room temperature as follows: a 5.0×10^{-3} M solution of $[\mathbf{2}][\text{BF}_4]$ in $\text{CH}_2\text{Cl}_2/[\text{N}^i\text{Bu}_4][\text{PF}_6]$ was introduced into an EPR spectroelectrochemical cell under a deoxygenated argon atmosphere and the solution was electrolyzed at constant potential ($E_w = -1.2$ V vs FeCp_2).

The obtained EPR spectrum (Fig. 4) consists of a broad signal (line width = 6.6 G) at $g_{\text{iso}} = 1.9773$, and is in good agreement with the spectrum computed for $[\mathbf{2}]^*$ (Fig. 5A), corresponding to a situation in which the electron density is almost localized at the two iron atoms Fe1 (0.4299) and Fe2 (0.6681).

This feature resembles to what was previously reported for diiron μ -alkylidene complexes of the type $[\text{Fe}_2\text{Cp}_2(\text{CO})_2(\mu\text{-CO})\{\mu\text{-C}(\text{CN})(\text{X})\}]^{n+}$ (X = H, C-, N-, O- or P-substituent), undergoing mono-electron reduction to the corresponding paramagnetic, dinuclear derivatives. In every cases, EPR spectroscopy indicated that the unpaired electron resided mainly on the Fe–Fe moiety [9a].

Table 1
Selected bond lengths (Å) and angles ($^\circ$) for **1c**.

Fe(1)–Fe(2)	2.561(2)	C(12)–Fe(1)	1.752(10)
C(11)–Fe(2)	1.915(12)	C(11)–Fe(1)	1.942(10)
C(13)–Fe(1)	1.939(10)	C(13)–Fe(2)	2.009(10)
C(14)–Fe(2)	2.114(9)	C(15)–Fe(2)	1.895(9)
C(11)–O(11)	1.188(12)	C(12)–O(12)	1.148(10)
C(13)–C(14)	1.442(13)	C(14)–C(15)	1.463(12)
C(15)–O(1)	1.210(10)	C(14)–C(16)	1.487(13)
Fe(2)–C(11)–Fe(1)	83.2(5)	O(12)–C(12)–Fe(1)	176.2(8)
Fe(1)–C(13)–Fe(2)	80.9(4)	C(14)–C(13)–Fe(1)	122.5(7)
C(13)–C(14)–C(15)	112.0(8)	C(14)–C(15)–Fe(2)	76.8(5)
O(1)–C(15)–C(14)	136.2(9)	O(1)–C(15)–Fe(2)	146.7(8)



Scheme 3.

The reaction of $[\mathbf{2}][\text{BF}_4]$ (ca. 0.60 mmol) with equimolar amount of CoCp_2 (in THF or CH_2Cl_2) afforded a mixture of non identified products, with prevalence of $[\text{Fe}_2\text{Cp}_2(\text{CO})_4]$ (isolated in ca. 30% yield). This evidence suggests that the dinuclear complex $[\mathbf{2}]^*$ is the initial product of the mono-electron reduction of $[\mathbf{2}][\text{BF}_4]$, but cleavage of the diiron frame may then take place to give, *inter alia*, the Fe(I) radical $[\text{FeCp}(\text{CO})_2]^*$, dimerizing to $[\text{Fe}_2\text{Cp}_2(\text{CO})_4]$. This observation puts some doubts on the attribution of the EPR spectrum (Fig. 4). Nevertheless it should be noted that the radical complex $[\text{FeCp}(\text{CO})_2]^*$ appeared EPR silent, except at low temperature in the presence of O_2 or radical trappers [11]. In these conditions, the EPR resonance was seen at g_{iso} value not corresponding to that of the spectrum in Fig. 4.

Furthermore, it is noteworthy that diiron complexes similar to $[\mathbf{2}]^+$, based on the $[\text{Fe}_2\text{Cp}_2(\text{CO})_2]$ core, undergo mono-electronic reduction affording still dinuclear compounds detected by EPR at room temperature [9a].

According to these considerations, we conclude that the EPR signal, detected in the course of the mono-electron reduction of $[\mathbf{2}][\text{BF}_4]$, could be reasonably assigned to a dinuclear Fe(I)–Fe(II) complex ($[\mathbf{2}]^*$), rather than to a following mononuclear Fe(I) product.

The main geometric parameters calculated for $[\mathbf{2}]^+$ and $[\mathbf{2}]^*$ are listed in Table 2, together with those obtained experimentally for $[\mathbf{2}]^+$ in the solid state [4].

A reading of Table 2 indicates the good agreement between the values related to $[\mathbf{2}]^+$ in the gas phase and the corresponding X-ray values obtained experimentally for the solid state [4]. Furthermore, the salient bond distances and angles concerning the μ -allenyl ligand do not significantly vary on going from $[\mathbf{2}]^+$ to $[\mathbf{2}]^*$. In other words, the allenyl ligand comes almost unaltered, in terms of both geometric features and coordination fashion, after mono-electron addition to the cation $[\mathbf{2}]^+$. In fact the only noticeable variation seems to be the elongation of the Fe–Fe interaction [from 2.6063(14) Å in $[\mathbf{2}][\text{BF}_4]$ (exp.) to 2.843 Å in $[\mathbf{2}]^*$ (calc.)]. These data

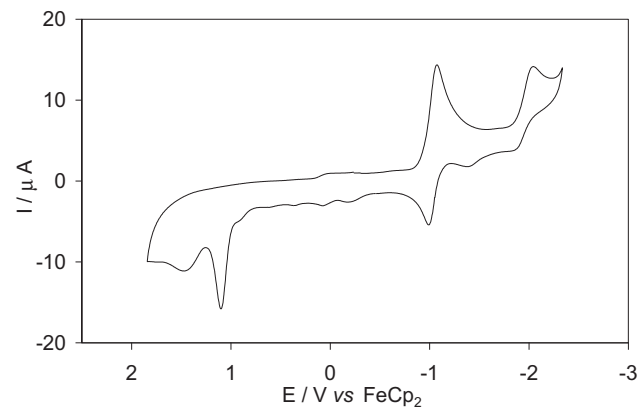


Fig. 2. Cyclic voltammogram of $[\mathbf{2}][\text{BF}_4]$ (2.0×10^{-3} M) recorded at a platinum electrode in CH_2Cl_2 solution containing $[\text{N}^i\text{Bu}_4][\text{PF}_6]$ 0.2 M. Scan rate = 0.1 V s^{-1} .

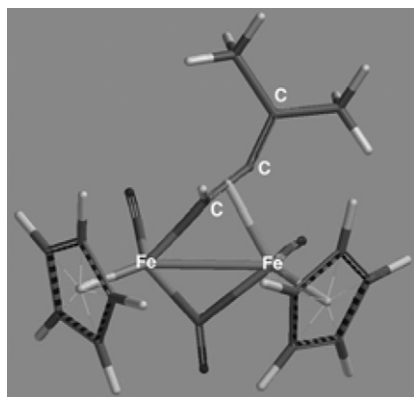


Fig. 3. DFT-calculated structure of $[2]^+$.

indicate that the unpaired electron in $[2]^•$ is localized prevalently at the metal centers Fe_1 and Fe_2 , coherently with the EPR evidences (see above). The elongation of the Fe–Fe bond on going from $[2]^+$ to $[2]^•$ gives a possible explanation for the formation of fragmentation products upon $CoCp_2$ reduction of $[2]^+$ (see above).

We have recently reported that the reduction of the μ -vinyl complex $[Fe_2Cp_2(CO)_2(\mu-CO)\{\mu-\eta^1:\eta^2-CH=CH(Ph)\}]^+$ (compound $[3]^+$, Scheme 4) generates a radical species with significant spin density located at the C_β carbon of the hydrocarbyl ligand. Computer analyses have suggested that the electron-withdrawing character of the phenyl group is crucial in order to allocate spin density on the vinyl chain. This leads to C–C coupling to give the stable $[Fe]_4$ bis-alkylidene complex $[Fe_2Cp_2(CO)_2(\mu-CO)\{\mu-CHCH(Ph)\}]_2$ [7], see Scheme 4.

In order to understand the influence of the allenyl substituents on the spin density distribution in the related radical complexes, the DFT structures of $[Fe_2Cp_2(CO)_2(\mu-CO)\{\mu-\eta^1:\eta^2_{\alpha,\beta}-C_\alpha H=C_\beta=C(R^1)(R^2)\}]^•$ ($R^1=R^2=H$, $[4]^•$; $R^1=H$, $R^2=Ph$, $[5]^•$; $R^1=R^2=Ph$, $[6]^•$) were optimized for the gas phase. The spin density distributions calculated for $[4]^•$ – $[6]^•$ are represented in Fig. 5. Like in complex $[2]^•$, the spin density in $[4]^•$ – $[6]^•$ is almost localized at the iron atoms: this means that the presence of phenyl substituents on the terminal carbon of the allenyl chain is ineffective to stabilize some spin density on carbon atoms, thus no C–C coupling reaction should be expected for $[2]^•$, $[4]^•$ – $[6]^•$.

Moreover the spin density maps of $[2]^•$ and $[6]^•$ provide a possible explanation for the outcomes of the reactions of $[Fe_2Cp_2(CO)_2(\mu-CO)\{\mu-\eta^1:\eta^2_{\alpha,\beta}-C_\alpha H=C_\beta=C(R^1)(R^2)\}]^+$ ($R^1=R^2=Me$, $[2]^+$; $R^1=R^2=Ph$, $[6]^+$) with strong nucleophiles (Nu^-) [4]. In fact these

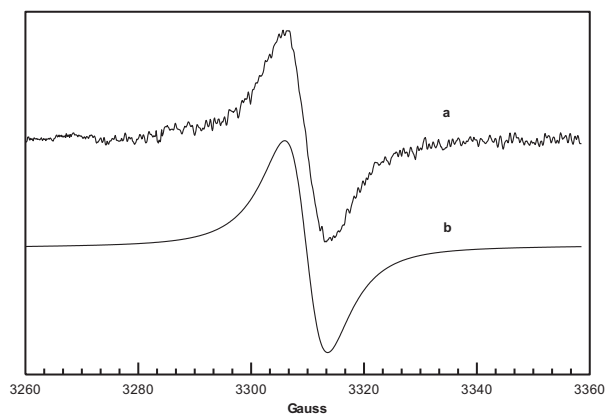


Fig. 4. EPR spectrum obtained by electrochemical mono-electron reduction of $[2][BF_4]$ (a: experimental; b: calculated).

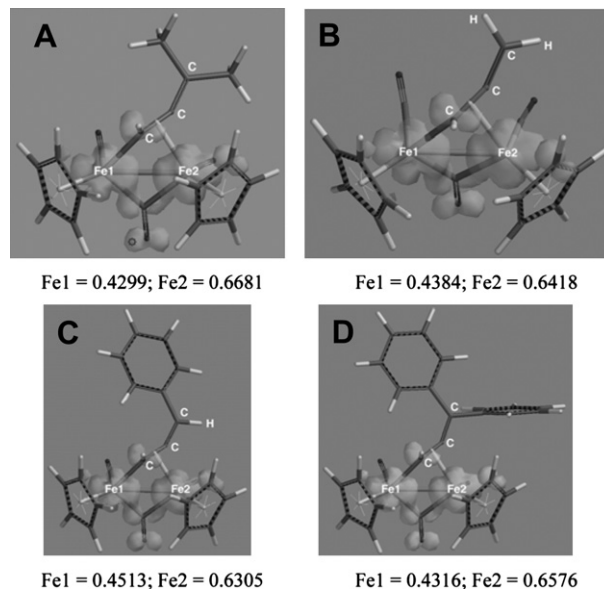


Fig. 5. DFT-calculated spin density (positive spin density, 0.002 electron au^{-3}) of $[2]^•$ (A) and $[Fe_2Cp_2(CO)_2(\mu-CO)\{\mu-\eta^1:\eta^2_{\alpha,\beta}-C_\alpha H=C_\beta=C(R^1)(R^2)\}]^•$ [$R^1=R^2=H$, $[4]^•$ (B); $R^1=H$, $R^2=Ph$, $[5]^•$ (C); $R^1=R^2=Ph$, $[6]^•$ (D)]. The spin density values at the two iron centers are reported below each diagram, respectively.

reactions, which normally result in the formation of mononuclear derivatives, could proceed with initial reduction of the dinuclear cation, causing the weakening of the Fe–Fe interaction (see above).

3. Conclusions

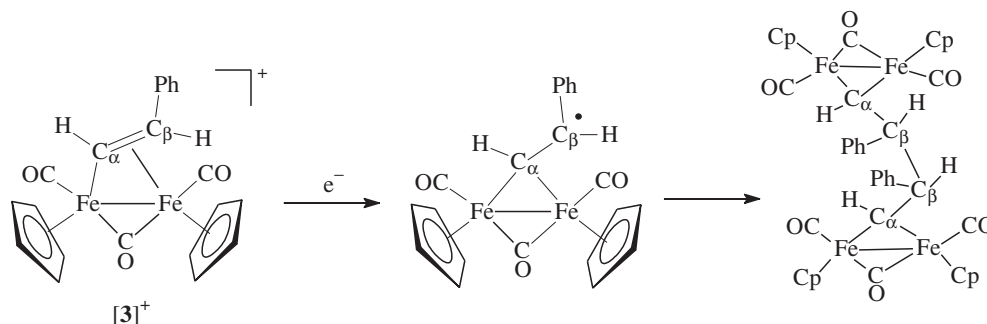
In this paper, we have reported some new aspects concerning the electrochemistry of dimetallacyclopentenone and μ -allenyl complexes based on the $[Fe_2Cp_2(CO)_2]$ core. Cationic diiron μ -allenyl complexes are subjected to easy mono-electron reduction affording initially a dinuclear derivative bearing the unpaired

Table 2
Selected bond lengths (Å) and angles ($^\circ$) for $[2]^+$ and $[2]^•$.

	$[2][BF_4]^a$	$[2]^+{}^b$	$[2]^•{}^b$
Fe_1-Fe_2	2.6063(14)	2.649	2.843
Fe_1-CO (terminal)	1.761(9)	1.784	1.754
Fe_1-CO (bridging)	1.815(9)	1.832	1.886
Fe_1-C_α	1.940(8)	1.936	1.943
Fe_2-CO (terminal)	1.766(10)	1.786	1.756
Fe_2-CO (bridging)	2.152(8)	2.107	2.021
Fe_2-C_α	2.026(8)	2.037	2.107
Fe_2-C_β	2.061(7)	2.128	2.125
$C_\alpha-C_\beta$	1.332(11)	1.361	1.359
$C_\alpha-CMe_2$	1.339(11)	1.331	1.330
$Fe_1-C_\alpha-C_\beta$	124.7(6)	128.12	130.48
$C_\alpha-C_\beta-CMe_2$	152.0(8)	153.10	152.50

^a Experimental values for the solid state (X-ray) [4].

^b Calculated values for the gas phase (DFT).



Scheme 4.

electron prevalently localized at the metal centers, independently on the nature of the allenyl substituents. This feature gives reason for the chemistry exhibited by cationic diiron μ -allenyl complexes, with particular reference to the non observed self-coupling of the radical generated by mono-electron reduction, in contrast with what found for analogous diiron Ph-substituted μ -vinyl species.

4. Experimental details

4.1. General

Reactions were carried out under nitrogen atmosphere, using standard Schlenk techniques. Glassware was oven-dried before use. Solvents were distilled before use under nitrogen from appropriate drying agents. Photolysis reactions were carried out in silica glass tubes by using a 150 W mercury lamp. Chromatography separations were carried out on columns of alumina (Fluka, Brockmann Activity I). All reactants were commercial products (Aldrich) of the highest purity available and used as received. Compounds $[\text{Fe}_2\text{Cp}_2(\text{CO})_4]$ (Strem), and $[\text{N}^t\text{Bu}_4][\text{PF}_6]$ (Fluka, puriss. electrochemical grade) were commercial products used as received. Ferrocene (FeCp_2), prepared according to the literature [12], was purified by sublimation. Infrared spectra were recorded at 298 K on FT-IR Perkin–Elmer Spectrometer equipped with a UATR sampling accessory (solid samples). NMR measurements were performed at 298 K on Bruker Avance DRX400 instrument equipped with probe BBFO broad band. The chemical shifts for ^1H and ^{13}C NMR spectra were referenced to the non deuterated aliquot of the solvent; the spectra were fully assigned *via* DEPT experiments and $^1\text{H},^{13}\text{C}$ correlation measured through *gs*-HSQC and *gs*-HMBC experiments [13]. EPR analyses were recorded at 298 K by Varian (Palo Alto, CA, USA) E112 spectrometer operating at X band, equipped with Varian E257 temperature control unit and interfaced to IPC 610/P566C industrial grade Advantech computer, using acquisition board [14] and software package especially designed for EPR experiments [15]. Experimental EPR spectra were simulated by WINSIM 32 program [16]. DFT geometry optimization and calculation of the electron spin density distribution were performed by the parallel Linux version of Spartan '10 software [17]. We adopted the B3LYP (Becke, three-parameter, Lee–Yang–Parr) [18,19] exchange–correlation functional formulated with the Becke 88 exchange functional [20], the correlation functional of Lee, Yang and Parr [21] and the 6-31G** base functions set, which is appropriate for calculations of split-valence plus-polarization quality.

Apparatus and techniques for the electrochemical measurements and joint EPR experiments were previously described [7]. Electrochemical measurements were performed in 0.2 M CH_2Cl_2 solutions of $[\text{N}^t\text{Bu}_4][\text{PF}_6]$ as supporting electrolyte and all the potential values were referenced to the ferrocene/ferrocenium couple (ferrocene was used as internal reference).

4.2. Synthesis of $[\text{Fe}_2\text{Cp}_2(\text{CO})(\mu\text{-CO})\{\mu\text{-}\eta^1:\eta^3\text{-C}_\alpha\text{H}=\text{C}_\beta(\text{CH}_2\text{OH})\text{C}(=\text{O})\}]$ (**1a**)

A solution of $[\text{Fe}_2(\text{Cp})_2(\text{CO})_4]$ (12.0 g, 0.0339 mol) and $\text{HC}\equiv\text{CCH}_2\text{OH}$ (0.31 mol) in THF (ca. 150 mL) was irradiated with UV light for 96 h. Then the volatile materials were removed under vacuo, and the residue was dissolved in CH_2Cl_2 and charged on a short alumina pad. Elution with a mixture of acetone and methanol (1:1 v/v) afforded a green band corresponding to **1a**. The product was obtained as a brownish-green microcrystalline solid upon removal of the solvent. Yield: 5.30 g, 41%. Anal. Calcd. for $\text{C}_{16}\text{H}_{14}\text{Fe}_2\text{O}_4$: C, 50.31; H, 3.69. Found: C, 49.82; H, 3.80. IR (solid state): $\nu(\text{OH})$ 3410 (m-br), $\nu(\text{CO})$ 1953 (vs), 1787 (s), 1744 (m) cm^{-1} . ^1H NMR (CDCl_3) δ 12.16 (s, 1 H, C_βH); 5.04, 4.77 (s, 10 H, Cp); 4.46, 3.89 (m, 2 H, CH_2OH). $^{13}\text{C}\{^1\text{H}\}$ NMR (CDCl_3) δ 261.6 ($\mu\text{-CO}$); 235.2 ($\text{C}=\text{O}$); 210.3 ($\text{CO}_{\text{terminal}}$); 176.8 (C_α); 87.4, 85.8 (Cp); 77.2 (CH_2); 9.4 (C_β).

4.3. X-ray characterization of $[\text{Fe}_2\text{Cp}_2(\text{CO})(\mu\text{-CO})\{\mu\text{-}\eta^1:\eta^3\text{-C}(\text{H})=\text{C}(\text{Ph})\text{C}(=\text{O})\}]$ (**1c**)

Crystals of **1c** suitable for X-ray analysis were collected by storing a dichloromethane solution of **1c** layered with pentane at -30°C for 48 h. Crystal data and collection details for $[\text{Fe}_2\text{Cp}_2(\text{CO})(\mu\text{-CO})\{\mu\text{-}\eta^1:\eta^3\text{-C}(\text{H})=\text{C}(\text{Ph})\text{C}(=\text{O})\}]$ (**1c**) are reported in Table 3. The diffraction experiments were carried out on a Bruker Apex II diffractometer equipped with a CCD detector using Mo– $K\alpha$ radiation. Data were corrected for Lorentz polarization and

Table 3
Crystal data and experimental details for **1c**.

Formula	$\text{C}_{21}\text{H}_{16}\text{Fe}_2\text{O}_3$
<i>F</i> _w	428.04
<i>T</i> , K	294(2)
λ , Å	0.71073
Crystal system	Monoclinic
Space group	$P2_1/n$
<i>a</i> , Å	11.811(6)
<i>b</i> , Å	12.077(6)
<i>c</i> , Å	12.697(7)
β , °	104.292(5)
Cell volume, Å ³	1755.1(16)
<i>Z</i>	4
<i>D</i> _c , g cm ⁻³	1.620
μ , mm ⁻¹	1.670
<i>F</i> (000)	872
Crystal size, mm	0.18 × 0.15 × 0.11
θ limits, °	2.11–25.02
Reflections collected	9575
Independent reflections	3068 (<i>R</i> _{int} = 0.0709)
Data/restraints/parameters	3068/231/284
Goodness on fit on <i>F</i> ²	1.050
<i>R</i> ₁ [<i>I</i> > 2 σ (<i>I</i>)]	0.0770
<i>wR</i> ₂ (all data)	0.2174
Largest diff. peak and hole, e.Å ⁻³	1.108/−0.486

absorption effects (empirical absorption correction SADABS) [22]. Structures were solved by direct methods and refined by full-matrix least-squares based on all data using F^2 [23]. All non-hydrogen atoms were refined with anisotropic displacement parameters. H-atoms were placed in calculated positions, except H(13) which was located in the Fourier map and the C(13)–H(13) distance restrained to 0.97 Å (s.u. 0.01) during refinement. H-atoms were treated isotropically using the 1.2 fold U_{iso} value of the parent C-atoms. The Cp ligand bound to Fe(2) is disordered. Disordered atomic positions were split and refined isotropically using one occupancy parameter per disordered group. Similar U restraints (s.u. 0.01) were applied to the C and O atoms.

Acknowledgement

We thank the Ministero dell'Università e della Ricerca Scientifica e Tecnologica (MIUR) for financial support.

Appendix A. Supplementary Material

CCDC no. 819692 for **1c**; contains the supplementary crystallographic data for this paper. These data can be obtained free of charge from The Cambridge Crystallographic Data Centre via www.ccdc.cam.ac.uk/data_request/cif.

References

- [1] (a) L. Busetto, P.M. Maitlis, V. Zanotti, *Coord. Chem. Rev.* 254 (2010) 470; (b) L. Busetto, F. Marchetti, R. Mazzoni, M. Salmi, S. Zacchini, V. Zanotti, *Chem. Commun.* (2010) 3327; (c) L. Busetto, F. Marchetti, R. Mazzoni, M. Salmi, S. Zacchini, V. Zanotti, *Organometallics* 28 (2009) 3465; (d) L. Busetto, F. Marchetti, M. Salmi, S. Zacchini, V. Zanotti, *Eur. J. Inorg. Chem.* (2008) 2437; (e) V.G. Albano, L. Busetto, F. Marchetti, M. Monari, S. Zacchini, V. Zanotti, *Organometallics* 26 (2007) 3448; (f) V.G. Albano, L. Busetto, F. Marchetti, M. Monari, S. Zacchini, V. Zanotti, *Organometallics* 22 (2003) 1326; (g) K. Boss, C. Dowling, A.R. Manning, *J. Organomet. Chem.* 509 (1996) 197; (h) E.L. Hoel, G.B. Ansell, S. Leta, *Organometallics* 5 (1986) 585; (i) M. Cooke, N.J. Forrow, S.A.R. Knox, *J. Chem. Soc. Dalton Trans.* (1983) 2435.
- [2] (a) F. Marchetti, S. Zacchini, M. Salmi, L. Busetto, V. Zanotti, *Eur. J. Inorg. Chem.* (2011) 1260; (b) L. Busetto, F. Marchetti, F. Renili, S. Zacchini, V. Zanotti, *Organometallics* 29 (2010) 1797; (c) L. Busetto, F. Marchetti, S. Zacchini, V. Zanotti, *Organometallics* 27 (2008) 5058; (d) L. Busetto, F. Marchetti, S. Zacchini, V. Zanotti, *Organometallics* 26 (2007) 3577; (e) L. Busetto, F. Marchetti, S. Zacchini, V. Zanotti, *Organometallics* 25 (2006) 4808; (f) L. Busetto, F. Marchetti, S. Zacchini, V. Zanotti, *Organometallics* 24 (2005) 2297; (g) V.G. Albano, L. Busetto, F. Marchetti, M. Monari, S. Zacchini, V. Zanotti, *Organometallics* 23 (2004) 3348.
- [3] A.F. Dyke, S.A.R. Knox, P.J. Naish, G.E. Taylor, *J. Chem. Soc. Dalton Trans.* (1982) 1297.
- [4] A. Boni, F. Marchetti, G. Pampaloni, S. Zacchini, *Dalton Trans.* (2010) 10866.
- [5] S.A.R. Knox, F. Marchetti, *J. Organomet. Chem.* 692 (2007) 4119.
- [6] A.F. Dyke, S.A.R. Knox, P.J. Morris, P.J. Naish, *J. Chem. Soc. Dalton Trans.* (1983) 1417.
- [7] A. Boni, T. Funaioli, F. Marchetti, G. Pampaloni, C. Pinzino, S. Zacchini, *Organometallics* 30 (2011) 4115.
- [8] The treatment of a solution of **1a** with equimolar amount of $\text{HBF}_4/\text{Et}_2\text{O}$ gave a red solid after work-up. IR analysis (in CH_2Cl_2) of the product was coherent with the formation of $[\text{Fe}_2\text{Cp}_2(\text{CO})_2(\mu\text{-CO})\{\mu\text{-}\eta^1\text{:}\eta^2_{\alpha,\beta}\text{-C}_2\text{H}=\text{C}_\beta=\text{CH}_2\}][\text{BF}_4]$ [bands at ν 2029vs ($\text{CO}_{\text{terminal}}$), 2009 m ($\text{CO}_{\text{terminal}}$), 1860 m ($\mu\text{-CO}$) cm^{-1}]. ^1H and ^{13}C NMR spectra (CDCl_3 , -50°C) evidenced the presence of more than one set of resonances, which could not be assigned.
- [9] (a) S. Bordoni, L. Busetto, F. Calderoni, L. Carlucci, F. Laschi, P. Zanello, V. Zanotti, *J. Organomet. Chem.* 496 (1995) 27; (b) V. Zanotti, S. Bordoni, L. Busetto, L. Carlucci, A. Palazzi, R. Serra, V.G. Albano, M. Monari, F. Prestopino, F. Laschi, P. Zanello, *Organometallics* 14 (1995) 5232; (c) M. Etienne, J. Talarmin, L. Toupet, *Organometallics* 11 (1992) 2058; (d) N.C. Schroeder, R.J. Angelici, *J. Am. Chem. Soc.* 108 (1986) 3688.
- [10] P. Zanello, *Inorganic Electrochemistry. Theory, Practice and Application*. RSC, Cambridge, U.K, 2003.
- [11] W.E. Lindsell, P.N. Preston, *J. Chem. Soc. Dalton Trans.* (1979) 1105.
- [12] G. Wilkinson, *Org. Syn* 36 (1956) 470.
- [13] W. Willker, D. Leibfritz, R. Kerssebaum, W. Bermel, *Magn. Reson. Chem.* 31 (1993) 287.
- [14] R. Ambrosetti, D. Ricci, *Rev. Sci. Instrum.* 62 (1991) 2281.
- [15] C. Pinzino, C. Forte, *EPR-ENDOR, ICQEM-CNR Rome, Italy*, 1992.
- [16] D.R. Duling, *J. Magn. Reson. B.* 104 (1994) 105.
- [17] Spartan '10, Wavefunction, Inc. 18401 Von Karman Avenue, Suite 370 Irvine, CA 92612 U.S.A.
- [18] K. Kim, K.D. Jordan, *J. Phys. Chem.* 98 (1994) 10089.
- [19] P.J. Stephens, F.J. Devlin, C.F. Chabalowski, M.J. Frisch, *J. Phys. Chem.* 98 (1994) 11623.
- [20] A.D. Becke, *Phys. Rev., A.* 38 (1988) 3098.
- [21] C. Lee, W. Yang, R.G. Parr, *Phys. Rev., B.* 37 (1988) 785.
- [22] G.M. Sheldrick, *SADABS, Program for Empirical Absorption Correction*. University of Göttingen, Germany, 1996.
- [23] G.M. Sheldrick, *SHELX97-Program for the refinement of crystal structure*. University of Göttingen, Germany, 1997.